SCIENTIFIC OASIS

Journal of Operations Intelligence

Journal homepage: www.jopi-journal.org
ISSN: 3009-4267

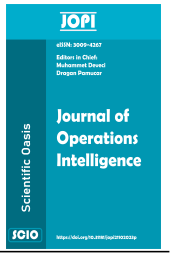

Anti-swing Control for Underactuated Crane under Disturbances

Tong Song[1,3], Juan Guo[2,*]

[1] School of Mathematics Science Liaocheng University, Liaocheng, Shandong 252000, China
[2] Guizhou City Vocational College, Guiyang, Guizhou 550025, China
[3] No.3 Middle School of Qihe, Dezhou, Shandong 251100, China

ARTICLE INFO

Article history:
Received 19 January 2025
Received in revised form16 March 2025
Accepted 27 April 2025
Available online 13 May 2025

Keywords:
Anti-swing Control; Underactuated Crane; Disturbances; Stability

ABSTRACT

In practical applications, a crane must achieve both precise positioning and effective suppression of swing. However, these dual requirements often present a contradiction: the acceleration and deceleration of the trolley may induce oscillations in the swing angle. This phenomenon stems from the inherent complexity of crane dynamics. On the one hand, cranes exhibit underactuated characteristics, as only the trolley is equipped with an actuator, while no direct actuator controls the swing angle. On the other hand, cranes possess highly coupled nonlinear dynamics, where actuated and unactuated variables interact, increasing the complexity of control design. To address these challenges, this paper investigates anti-swing control for an overhead crane under disturbances. The proposed approach suppresses swing by coupling its integral information with the trolley position and introducing negative damping into the unactuated subsystem. To handle disturbances, both matched and mismatched disturbances are incorporated into the control channel and compensated through feedforward mechanisms. Theoretical analysis demonstrates that the designed control system is stable. Simulation results validate the effectiveness of the proposed approach.

1. Introduction

Cranes are a well-known class of nonlinear underactuated systems, with overhead cranes widely used due to their relatively simple structure. Structurally, an overhead crane consists of a rail, a trolley, and a suspended rope [1–4]. Minimizing payload swing during trolley motion is crucial for ensuring operational safety.

The current researches on crane control can be classified into open-loop control and closed-loop

*Corresponding author.
E-mail address: jguo1385@163.com

https://doi.org/10.31181/jopi31202543

control methods. For open-loop control methods, typical examples include input shaping and trajectory planning [5–8]. The closed-loop control methods, including sliding mode control [9, 10], flatness-based control [11, 12], and energy-based (passivity-based) control [13–15], have consistently played a key role in addressing the anti-swing issue of cranes. In the studies of SMC, actuated and unactuated states were typically to form sliding variable. The idea behind this is to enhance the dynamic behavior between driving and non-driving variables through coupling. This treatment can also be found in energy-based approaches. Researchers argue that this enhancement can improve control performance and effectively suppress payload oscillations.

The cranes are often deployed in complex environments, such as factories and ports, often face various disturbances. However, most of these methods exhibit limited robustness when cranes suffer from disturbances, especially mismatched disturbances. In overhead cranes, robustness in this context refers to the ability to suppress payload oscillations while maintaining precise trolley positioning. For example, when wind-induced swing is significant, the trolley should respond swiftly to mitigate oscillations. When external disturbances subside, it should restore positioning accuracy without compromising swing suppression. At present, extensive research on crane control has aimed to enhance robustness by mitigating disturbance effects. For example, the works of [16] and [17] used adaptive approach to deal with the unknown disturbance. It should be note that disturbance observer (DO)-based control algorithms have also received significant attention in the literature. Many types of disturbance observers have been proposed for overhead cranes, including extended state observers [18], nonlinear disturbance observers [19], and fixed-time disturbance observers [20]. However, the above approaches primarily address matched disturbances, while suppression of unmatched disturbances remains largely unexplored.

Motivated by the above discussions, this work focus on the anti-swing strategy for overhead cranes under matched and mismatched disturbances. The main contributions of this paper are summarized in the following:

1) A sufficient condition for stabilizing the unactuated variable is proposed, and from which, an auxiliary signal capable of attenuating the swing angle is derived.

2) The proposed controller includes an effective disturbance compensation term to reduce the effect disturbances, forcing the trolley to follow the desired translational motion asymptotically.

3) Different from the existing control methods, an important feature of this method is that the attenuation property of swing angle can be maintained even under mismatched disturbances such as wind disturbances.

2. Model Description and Problem formulation

The underactauted crane system considered in this paper is shown in Fig.1, whose dynamic is described as

$$\begin{aligned}(M+m)\ddot{x}+ml\ddot{\theta}\cos(\theta)-ml\dot{\theta}^2\sin(\theta)&=F_u+F_r+\omega_1,\\ ml^2\ddot{\theta}+ml\cos(\theta)\ddot{x}+mgl\sin(\theta)&=-d_\theta\dot{\theta}+\omega_2,\end{aligned}\tag{1}$$

where M and m represent the trolley mass and the payload mass, l denotes the rope length, and g is the gravity acceleration. x and θ denote the trolley position and the swing angle of the rope, respectively. F_u is the control torque to be designed, and ω_1 and ω_2 are the wind disturbance applied horizontally on the trolley and payload, respectively. Meanwhile, F_r is the friction, modeled by

$$F_r=-f_0\tanh(\dot{x}/v_0)+f_1|\dot{x}|\dot{x},$$

where f_0, v_0, and f_1 are friction-related parameters.

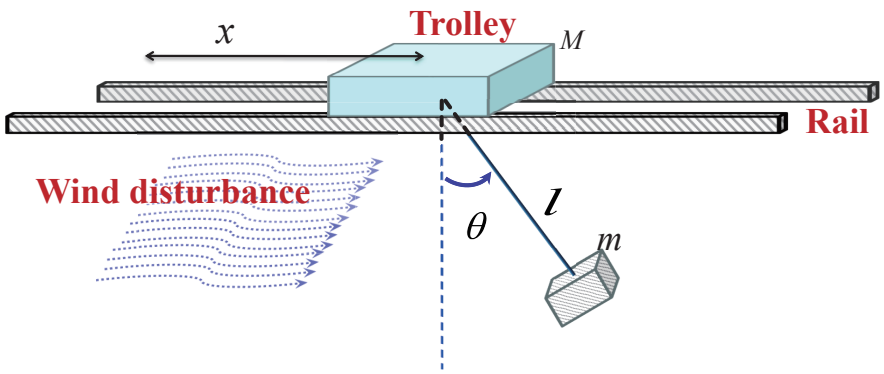

Fig. 1 Schematic illustration of a crane system.

The control goal is to make the trolley move to the desired potion p_d while suppressing rope swing. To proceed, the following assumption is needed.

Assumption 1: The wind disturbance ω_i $(i = 1, 2)$ satisfy $|\omega_i| \leq \omega_{0i}$, $|\dot{\omega}_i| \leq \omega_{i1}$, and $|\ddot{\omega}_i| \leq \omega_{i2}$, where ω_{0i}, ω_{1i}, and ω_{2i} are known positive constants.

Assumption 2: $-\frac{\pi}{3} \leq \theta \leq \frac{\pi}{3}$.

Assumption 3: The initial condition satisfy $\dot{x}(0) = 0$, $\theta(0) = 0$, and $\dot{\theta}(0) = 0$.

3. Controller design and Main results

3.1 Sufficient conditions for stabilizing unactuated state

Let us regard the dynamic of $\dot{\theta}$ as a subsystem and consider the sufficient conditions for stabilizing θ. Define $S = x - x_d - \lambda$ with x_d and λ being designed as

$$x_d = \begin{cases} (p_d - x(0))\left(\frac{t}{t_d} - \frac{\sin(2\pi t/t_d)}{2\pi}\right) + x(0), 0 \leq t \leq t_d, \\ p_d, \ t \geq t_d. \end{cases}$$

$$\lambda = k_f e^{-\mu t} \int_0^t \sin(\theta) d\tau,$$

where $t_d > 0$, $k_f > 0$ and $\mu > 0$. From (1), one has

$$\ddot{\theta} = -\frac{\cos(\theta)}{l}(\ddot{S} + \ddot{\lambda} + \ddot{x}_d) - \frac{g}{l}\sin(\theta) + \frac{\omega_2 - d_\theta \dot{\theta}}{ml^2}, \tag{2}$$

which leads to the following proposition.

Proposition 1: If the auxiliary signals S satisfy $\ddot{S} \in L_\infty$ and $\ddot{S} \in L_2$, then one obtains $\dot{\theta} \to 0$ and $\theta \to 0$.

Proof: Introducing $\zeta_1 = \theta$ and $\zeta_2 = \dot{\theta}$ converts (2) to the cascade form as

$$\begin{aligned} \dot{\zeta}_1 &= \zeta_2, \\ \dot{\zeta}_2 &= -\frac{\cos(\zeta_1)}{l}(\ddot{S} + \ddot{\lambda} + \ddot{x}_d) - \frac{g}{l}s_1 + \frac{\omega_2 - d_\theta \zeta_2}{ml^2}. \end{aligned} \tag{3}$$

Since $S \equiv 0$, one has $\ddot{S} = 0$. For simplicity, denote $s_1 = \sin(\zeta_1), c_1 = \cos(\zeta_1)$, $\lambda_1 = \mu^2 \int_0^t s_1 d\tau$ and $\lambda_2 = -2\mu s_1$. Then, it follows that $\ddot{\lambda} = k_f e^{-\mu t}\lambda_1 + k_f e^{-\mu t}\lambda_2 + k_f e^{-\mu t} c_1\zeta_2$. In the sequel, one considers the following Lyapunov function

$$V_\theta = \frac{1}{2}\zeta_2^2 + \frac{g}{l}(1 - c_1),$$

whose derivative is

$$\dot{V}_\theta = -\frac{1}{l}\big(k_f e^{-\mu t} c_1^2 + \frac{d_\theta}{ml}\big)\zeta_2^2 - \frac{\ddot{S}}{l} c_1\zeta_2 - \frac{k_f}{l} c_1\zeta_2 e^{-\mu t}(\lambda_1 + \lambda_2) + \frac{\omega_2}{ml^2}\zeta_2 - \frac{\ddot{x}_d}{l} c_1\zeta_2. \tag{4}$$

Using Young's inequality, it can be calculated that

$$\begin{aligned}
-\frac{k_f}{l} c_1\zeta_2 e^{-\mu t}\lambda_1 &\le \frac{k_f}{4l} e^{-\mu t} c_1^2\zeta_2^2 + \frac{k_f}{l} e^{-\mu t}\lambda_1^2,\\
-\frac{k_f}{l} c_1\zeta_2 e^{-\mu t}\lambda_2 &\le \frac{k_f}{4l} e^{-\mu t} c_1^2\zeta_2^2 + \frac{k_f}{l} e^{-\mu t}\lambda_2^2,\\
-\frac{\ddot{x}_d}{l} c_1\zeta_2 &\le \frac{k_f}{4l} e^{-\mu t} c_1^2\zeta_2^2 + \frac{\ddot{x}_d^2}{l} e^{\mu t} \le \frac{k_f}{4l} e^{-\mu t} c_1^2\zeta_2^2 + \frac{e^{\mu t_d}}{l}\ddot{x}_d^2,
\end{aligned}$$

and

$$\begin{aligned}
-\frac{\ddot{S}}{l} c_1\zeta_2 &\le \frac{3d_\theta}{8ml^2}\zeta_2^2 + \frac{2m}{3d_\theta}\ddot{S}^2,\\
\frac{\omega_2}{ml^2}\zeta_2 &\le \frac{3d_\theta}{8ml^2}\zeta_2^2 + \frac{2}{3d_\theta ml^2}\omega_2^2.
\end{aligned}$$

Thus, (4) can be upper bounded as

$$\dot{V}_\theta \le -\frac{1}{4l}\big(k_f e^{-\mu t} c_1^2 + \frac{d_\theta}{ml}\big)\zeta_2^2 + \frac{k_f}{l} e^{-\mu t}\lambda_1^2 + \frac{k_f}{l} e^{-\mu t}\lambda_2^2 + \frac{2}{3d_\theta ml^2}\omega_2^2 + \frac{e^{\mu t_d}}{l}\ddot{x}_d^2 + \frac{2m}{3d_\theta}\ddot{S}^2. \tag{5}$$

Since $\ddot{S} \in L_\infty$, there exists a constants such that $|\ddot{S}| \le \bar{S}$. Note that

$$\begin{aligned}
\frac{k_f}{l} e^{-\mu t}\lambda_1^2 &\le \frac{k_f}{l} e^{-\mu t}\mu^4 t^2 \le \frac{4k_f\mu^2}{le^2},\\
\frac{k_f}{l} e^{-\mu t}\lambda_2^2 &\le \frac{4k_f}{l} e^{-\mu t}\mu^2 \le \frac{4k_f\mu^2}{l},\\
\ddot{x}_d^2 \le \frac{4\pi^2 p_d^2}{t_d^4} &\Rightarrow \frac{e^{\mu t_d}}{l}\ddot{x}_d^2 \le \frac{e^{\mu t_d} 4\pi^2 p_d^2}{l t_d^4}.
\end{aligned}$$

Then, (5) can be rewritten as

$$\dot{V}_\theta \le -\frac{1}{4l}\big(k_f e^{-\mu t} c_1^2 + \frac{d_\theta}{ml}\big)\zeta_2^2 + \Delta, \tag{6}$$

where $\Delta = \frac{4k_f\mu^2}{le^2} + \frac{4k_f\mu^2}{l} + \frac{2\omega_{02}^2}{3d_\theta ml^2} + \frac{e^{\mu t_d} 4\pi^2 p_d^2}{l t_d^4} + \frac{2m}{3d_\theta}\bar{S}^2$. Therefore, it can be further obtained that $|\zeta_2| \le \sqrt{\frac{4ml^2\Delta}{d_\theta}}$, i.e. $\zeta_2 \in L_\infty$.

In addition, after some simple calculations, the following inequalities can be established

$$\begin{aligned}\frac{k_f}{l}\int_0^t e^{-\mu\tau}\mu^4\tau^2 d\tau &= -\frac{k_f\mu^3}{l}e^{-\mu t}t^2 - \frac{2k_f\mu^2}{l}e^{-\mu t}t - \frac{2k_f\mu}{l}e^{-\mu t} + \frac{2k_f\mu}{l} \\ &\leq \frac{4k_f\mu}{le^2} + \frac{2k_f\mu}{le} + \frac{2k_f\mu}{l} \quad , \\ \frac{4k_f\mu^2}{l}\int_0^t e^{-\mu\tau}d\tau &= \frac{4k_f\mu^2}{l}(-\frac{1}{\mu}e^{-\mu t} + \frac{1}{\mu}) \leq \frac{4k_f\mu}{l}.\end{aligned} \tag{7}$$

Integrating (5) from 0 to t leads to the fact that

$$\begin{aligned}V_\theta + \frac{1}{4l}\int_0^t \big(k_f e^{-\mu\tau}\cos^2(\zeta_1) + \frac{d_\theta}{ml}\big)\zeta_2^2 d\tau \leq \int_0^t \frac{k_f}{l}e^{-\mu\tau}\lambda_1^2 d\tau + \int_0^t \frac{k_f}{l}e^{-\mu\tau}\lambda_2^2 d\tau \\ + \frac{2}{3d_\theta ml^2}\int_0^t \omega_2^2 d\tau + \frac{e^{\mu t_d}}{l}\int_0^t \ddot{x}_d^2 d\tau,\end{aligned}$$

which means

$$\begin{aligned}\frac{d_\theta}{4ml^2}\int_0^t \zeta_2^2 d\tau &\leq \frac{k_f}{l}\int_0^t e^{-\mu\tau}\mu^4\tau^2 d\tau + \frac{4k_f\mu^2}{l}\int_0^t e^{-\mu\tau}d\tau + \frac{2}{3d_\theta ml^2}\int_0^t \omega_2^2 d\tau + \frac{e^{\mu t_d}}{l}\int_0^t \ddot{x}_d^2 d\tau \\ &\leq \frac{4k_f\mu}{le^2} + \frac{2k_f\mu}{le} + \frac{6k_f\mu}{l} + \frac{2}{3d_\theta ml^2}\int_0^t \omega_2^2 d\tau + \frac{e^{\mu t_d}}{l}\int_0^t \ddot{x}_d^2 d\tau < +\infty.\end{aligned}$$

Therefore, one obtains $\zeta_2 \in L_2$. Since $\zeta_2 \in L_\infty$, one knows $\ddot{\lambda} \in L_\infty \Rightarrow \dot{\zeta}_2 \in L_\infty$. Based on the Barbalat's Lemma, we have $\zeta_2 \to 0$. In addition, it is not hard to figure out that $0 \leq |\ddot{\lambda}| \leq k_f\mu^2 e^{-\mu t}t + 2k_f\mu e^{-\mu t} + k_f e^{-\mu t}|\zeta_2|f(t)$. Bearing $f(t) \to 0$ and $|\ddot{\lambda}| \geq 0$ in mind, one can easily find $\ddot{\lambda} \to 0$.

Further, let

$$\bar{g} = \zeta_2, g_0 = -\frac{g}{l}s_1,\ g_1 = -\frac{c_1}{l}\ddot{\lambda} + \frac{\omega_2}{ml^2} - \frac{d_\theta\zeta_2}{ml^2}.$$

Recalling (3), it yields that

$$\dot{\bar{g}} = g_0 + g_1,$$

where g_0 and g_1 satisfy $\dot{g}_0 = -\frac{g}{l}c_1\zeta_2 \in L_\infty$ and $g_1 \to 0$. Then utilizing the Extended Barbalat's Lemma get $\dot{\bar{g}} \to 0$, which implies $g_0 \to 0 \Rightarrow \zeta_1 \to 0$.

Clearly, if k_f is set as $k_f = 0$, then $\lambda \equiv 0$. The results in Proposition 1 can also be derived using the similar procedure in above proof, except that (6) becomes

$$\dot{V}_\theta \leq -\frac{1}{4l}\big(\frac{d_\theta}{ml}\big)\zeta_2^2 + \Delta. \tag{8}$$

In this scenario, the convergence of the unactuated state only depends on the physical parameters of the system itself, including payload mass m, rope length l, and damping parameter d_θ. In other words, the inserting of positive k_f and μ in (6) increases the negative damping of subsystem 3, which is helpful to enhance the anti-swing ability under wind disturbance. In the next subsection, we will illustrate the damping injection.

3.2 Controller design

By combining S, (2) and the first equation of (1), it obtains that

$$\ddot{S} = \frac{1}{\bar{M}}u + h(x, \dot{x}, \theta, \dot{\theta}, t) + \frac{1}{\bar{M}}d(\theta, t), \tag{9}$$

where

$$\begin{aligned} h &= -(\ddot{x}_d + \ddot{\lambda}) + \frac{1}{\bar{M}}\left(mg\sin(\theta)\cos(\theta) + \frac{d_\theta}{l}\cos(\theta)\dot{\theta} + ml\dot{\theta}^2\sin(\theta)\right), \\ d &= \omega_1 - \frac{\omega_2}{l}\cos(\theta) + F_r, \\ \bar{M} &= M + m\sin^2(\theta), u = F_u. \end{aligned} \tag{10}$$

The speed and acceleration of the rope are always bounded due to its physical structure. Therefore, the following assumption is reasonable:

Assumption 4: $|\dot{\theta}| \leq \theta_1$ (r/s), $|\ddot{\theta}| \leq \theta_2$ (r/s^2).

For practical applications, it is often not difficult to develop sufficiently large bounds on d, $\dot{d}$, and $\ddot{d}$. Specifically, one has $|d| \leq \omega_{01} + \frac{\omega_{02}}{l}d_0$, $|\dot{d}| \leq \omega_{11} + \frac{g\omega_{02}}{l} + \frac{\omega_{21}}{l}d_1$ and $|\ddot{d}| \leq \omega_{21} + \frac{g^2}{l}\omega_{02} + \frac{g}{l}\omega_{02} + \frac{g}{l}\omega_{21} + \frac{\omega_{22}}{l}d_2$.

Define two auxiliary signals as $z_1 = k_1 S + \dot{S}$ and $z_2 = k_2 z_1 + \dot{z}_1$ with $k_1 > 0$ and $k_2 > 0$. Subsequently, the controller is designed as

$$\begin{aligned} u &= F_u = -\bar{M}h - \hat{d} - \bar{M}(k_2 z_1 + k_1 \dot{S}), \\ \hat{d} &= k_3 \int_0^t k_2 z_1 d\tau + k_3 z_1 + k_4 \int_0^t sign z_1 d\tau + \int_0^t z_1 d\tau,\ \hat{d}(0) = 0, \end{aligned} \tag{11}$$

with the parameters satisfying

$$k_1 > \frac{1}{2}, k_2 > 1, k_3 > m\theta_1, k_4 > d_1 + \frac{d_2}{k_2 - 1}. \tag{12}$$

Now, let us summarize the main result of this paper.

Theorem 1: Consider system (1), under Assumptions 1-4, if the control law (11) with disturbance compensation term $\hat{d}$ is applied, then the position and swing angle satisfy $x \to p_d$ and $\theta \to 0$.

Proof: Before the proof of Theorem 1, we construct the auxiliary function as

$$\dot{J} = -J - z_2(\dot{d} - k_4 sign z_1),\ J(0) = 0. \tag{13}$$

First, one shows the positive definiteness of J. With the similar analysis, it can be known that

$$\begin{aligned} J &= k_4|z_1| - \dot{d}z_1 + \int_0^t e^{-(t-\tau)}L(\tau)d\tau, \\ L &= (k_2 - 1)(k_4|z_1| - z_1\dot{d}) + z_1\ddot{d}. \end{aligned} \tag{14}$$

Based on the fact $\dot{d}z_1 \leq d_1|z_1| \Rightarrow -\dot{d}z_1 \geq -d_1|z_1|$ and $-z_1\ddot{d} \leq d_2|z_1| \Rightarrow z_1\ddot{d} \geq -d_2|z_1|$, one further gets the following result

$$\begin{aligned} J &\geq (k_4 - d_1)|z_1| + e^{-t}\int_0^t e^{\tau}L(\tau)d\tau, \\ L &\geq (k_2 - 1)\big(k_4|z_1| - d_1|z_1|\big) - d_2|z_1| \geq \big((k_2 - 1)(k_4 - d_1) - d_2\big)|z_1|. \end{aligned} \tag{15}$$

Under the condition in (12), one obtains that

$$L \geq 0 \Rightarrow J \geq 0.$$

Thereafter, one considers the Lyapunov function as

$$V = \frac{1}{2}S^2 + \frac{1}{2}z_1^2 + \frac{\bar{M}}{2}z_2^2 + J. \tag{16}$$

Differentiating V, one obtains

$$\begin{aligned} \dot{V} =& S(z_1 - k_1 S) + z_1(z_2 - k_2 z_1) + \bar{M} z_2 \dot{z}_2 + \frac{\dot{M}}{2} z_2^2 + \dot{J} \\ =& -k_1 S^2 - k_2 z_1^2 + S z_1 + z_1 z_2 - \frac{\dot{M}}{2} z_2^2 - J + z_2(\dot{d} - \dot{\hat{d}}) - z_2(\dot{d} - k_4 sign z_1). \end{aligned} \tag{17}$$

Note that

$$\begin{aligned} \dot{\hat{d}} &= k_3 z_2 + k_4 sign z_1 + z_1, \\ |\dot{\bar{M}}| &= |2m \sin(\theta) \cos(\theta) \dot{\theta}| \leq 2m\theta_1. \end{aligned}$$

Then, after a simple substitution, it can be obtained that

$$\begin{aligned} \dot{V} &\leq -(k_1 - \frac{1}{2})S^2 - (k_2 - \frac{1}{2})z_1^2 - J - (k_3 - m\theta_1)z_2^2 \leq -kV \\ &\Rightarrow V \leq e^{-kt}V(0), \end{aligned} \tag{18}$$

in which $k = \min\{2k_1 - 1,\ 2k_2 - 1,\ \frac{2k_3 - 2m\theta_1}{M+m},\ 1\}$.

Therefore, it claims that

$$\begin{aligned} |S| &\leq \sqrt{2e^{-kt}V(0)} \leq \sqrt{2V(0)}, \\ |z_1| &\leq \sqrt{2e^{-kt}V(0)} \leq \sqrt{2V(0)}, \\ |z_2| &\leq \sqrt{2e^{-kt}V(0)} \leq \sqrt{2V(0)}. \end{aligned} \tag{19}$$

Further, from $z_2 = k_2 z_1 + \dot{z}_1$, we have $\ddot{S} = z_2 + k_1^2 S - (k_1 + k_2)z_1 \Rightarrow |\ddot{S}| \leq \bar{k}\sqrt{2V(0)}$ with $\bar{k} = 1 + k_1 + k_2 + k_1^2$. Meanwhile, it can be obtained that

$$\ddot{S}^2 \leq 2\bar{k}^2 e^{-kt}V(0) \Rightarrow \int_0^t \ddot{S}^2 d\tau \leq \frac{2\bar{k}^2}{k}V(0). \tag{20}$$

Then, applying proposition 1 knows $\theta \to 0$ and $x \to p_d$. The proof of Theorem 1 is completed.

4. Simulation verification

To validate the feasibility and effectiveness of the proposed approach, two cases of simulations are carried out. The physical parameters are $M = 200$ kg, $m = 20$ kg, $l = 5$ m and $g = 9.8$ m/s^2. The control parameters are $k_1 = k_2 = k_3 = 3$, $k_4 = 30$, $k_f = 1$, and $\mu = 0.3$. In the two cases of the simulations, the control parameters keep unchanged.

Case 1: The system is only disturbed by the following friction:

$$F_r = -5.4 \tanh(\dot{x}/0.1) + |\dot{x}|\dot{x};$$

Case 2: Besides the friction in *Case 1*, the system is disturbed by the extra disturbance:

$$d = 10 \sin(0.5\pi t),\ \omega_1 = \omega_2 = \begin{cases} 10(t-10)(t-20) & 10 \leq t \leq 20 \\ 0 & \text{others}. \end{cases} \tag{21}$$

The simulation results of *Case 1* are presented in Figs.2 and 3. Fig. 2 shows the trolley position x, swing angel θ, and control input F_u. It can be seen that the trolley can adjust the load to the desired position within about 10 s by tracking the time-varying signal x_d $(t_d = 8)$, and the swing angle is effectively confined to a small range. The effective control performance is attributed to the feedforward compensation of $\hat{d}$ for unknown friction, as illustrated in Fig. 3.

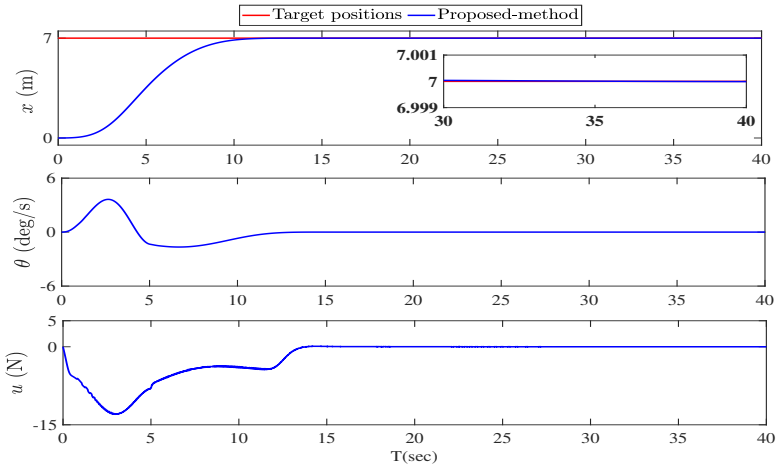

Fig. 2 System responses of Case 1.

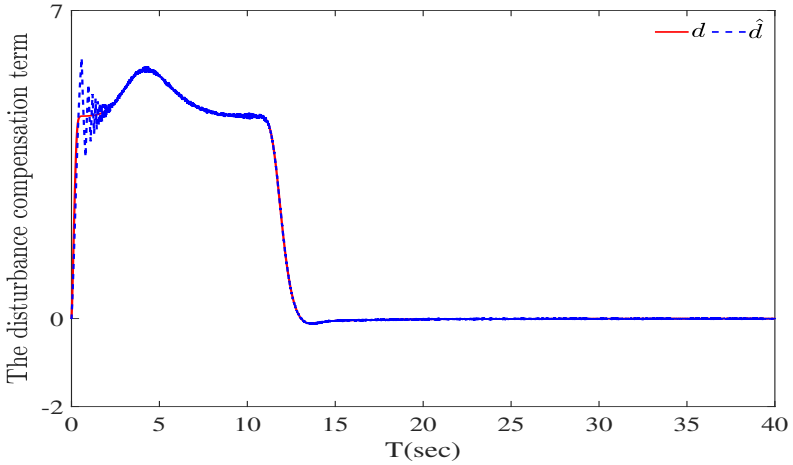

Fig. 3 Disturbance estimation of Case 1.

In Case 2, additional disturbances are introduced, with mismatched disturbances occurring between 10–20 s to simulate the wind disturbances. From Fig. 4, it can be seen that the trolley has been regulated to the desired position with the swing angel being also removed before 10 s. In the time interval 10-20, it can be seen that the controller made corresponding adjustments to eliminate the swing. Fig. 5 displays the efficient disturbance estimation.

5. Conclusion

This paper investigated the anti-swing control of an overhead crane under disturbances, addressing the dual challenge of precise positioning and swing suppression. The inherent underactuated na-

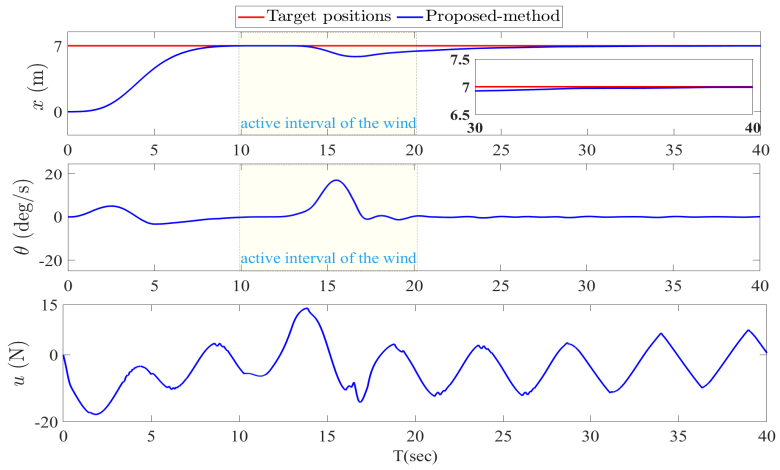

Fig. 4 System responses of Case 2.

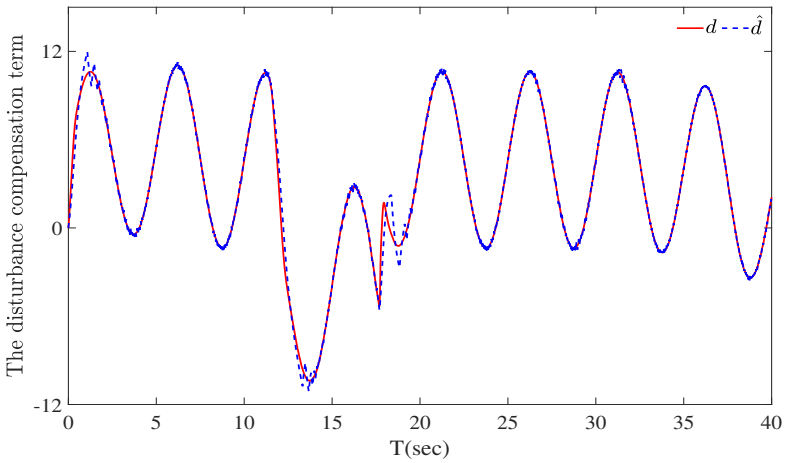

Fig. 5 Disturbance estimation of Case 2.

ture of the crane, along with its strong coupling between actuated and unactuated variables, complicates control design. To overcome these challenges, a control strategy was developed that integrates the integral information of the swing angle with the trolley position, effectively introducing negative damping into the unactuated subsystem. Additionally, the disturbances were compensated for through feedforward mechanisms. Theoretical analysis and simulation results validated the effectiveness of the proposed approach, demonstrating its potential for improving crane control performance in practical applications. Future research will focus on the cranes with double pendulum effects.

Author Contributions

Conceptualization, T.S. and J.G.; methodology, T.S. and J.H.; software, T.S.; validation, T.S. and J.G.; formal analysis, T.S. and J.G.; writing—original draft preparation, T.S. and J.G.; writing—review and editing, T.S. and J.G.; supervision, T.S. and J.G. All authors have read and agreed to the published version of the manuscript.

Funding

This research received no external funding.

Data Availability Statement

The datasets generated during and/or analyzed during the current study is available from the corresponding author on reasonable request.

Conflicts of Interest

The authors declare that they have no known competing financial interests or personal relationships that could have appeared to influence the work reported in this paper.

Acknowledgement

This research was not funded by any grant research.

References

[1] Hamdy, M., Shalaby, R., & Sallam, M. (2018). A hybrid partial feedback linearization and deadbeat control scheme for a nonlinear gantry crane. *Journal of the Franklin Institute*, *355*(14), 6286–6299. https://doi.org/10.1016/j.jfranklin.2018.06.014

[2] Huaitao, S., Fuxing, Y., Zhe, Y., Shenghao, T., Yinghan, T., & Gang, H. (2022). Research on nonlinear coupled tracking controller for double pendulum gantry cranes with load hoisting/lowering. *Nonlinear Dynamics*, *108*(1), 223–238. https://doi.org/10.1007/s11071-021-07185-6

[3] Lawrence, J. W. (2006). *Crane oscillation control: Nonlinear elements and educational improvements* [Doctoral dissertation, Georgia Institute of Technology.].

[4] Sun, N., & Fang, Y. (2014). Nonlinear tracking control of underactuated cranes with load transferring and lowering: Theory and experimentation. *Automatica*, *50*(9), 2350–2357. https://doi.org/10.1016/j.automatica.2014.07.023

[5] Chen, Q., Yu, S., Cheng, W., Zhang, M., Liu, J., Gao, L., Du, R., & Yan, W. (2023). Inverse motion planning method for overhead crane systems with state constraints. *Asian Journal of Control*, *25*(4), 2934–2946. https://doi.org/10.1002/asjc.2988

[6] Zhang, X., Fang, Y., & Sun, N. (2014). Minimum-time trajectory planning for underactuated overhead crane systems with state and control constraints. *IEEE Transactions on Industrial Electronics*, *61*(12), 6915–6925. https://doi.org/10.1109/TIE.2014.2320231

[7] Fang, Y., Ma, B., Wang, P., & Zhang, X. (2012). A motion planning-based adaptive control method for an underactuated crane system. *IEEE Transactions on Control Systems Technology*, *20*(1), 241–248. https://doi.org/10.1109/TCST.2011.2107910

[8] Zhang, M., & Jing, X. (2022). Adaptive neural network tracking control for double-pendulum tower crane systems with nonideal inputs. *IEEE Transactions on Systems, Man, and Cybernetics: Systems*, *52*(4), 2514–2530. https://doi.org/10.1109/TSMC.2020.3048722

[9] Wu, X., Xu, K., Lei, M., & He, X. (2020). Disturbance-compensation-based continuous sliding mode control for overhead cranes with disturbances. *IEEE Transactions on Automation Science and Engineering*, *17*(4), 2182–2189. https://doi.org/10.1109/TASE.2020.3015870

[10] Tuan, L. A. (2021). Neural observer and adaptive fractional-order backstepping fast-terminal sliding-mode control of rtg cranes. *IEEE Transactions on Industrial Electronics*, *68*(1), 434–442. https://doi.org/10.1109/TIE.2019.2962450

[11] Lobe, A., Ettl, A., Steinboeck, A., & Kugi, A. (2018). Flatness-based nonlinear control of a three-dimensional gantry crane [12th IFAC Symposium on Robot Control SYROCO 2018]. *IFAC - PapersOnLine*, *51*(22), 331–336. https://doi.org/10.1016/j.ifacol.2018.11.563

[12] Zhongcai, Z., Yuqiang, W., & Jinming, H. (2017). Differential-flatness-based finite-time anti-swing control of underactuated crane systems. *Nonlinear Dynamics*, *87*(3), 1749–1761. https://doi.org/10.1007/s11071-016-3149-7

[13] Zhao, B., Ouyang, H., & Iwasaki, M. (2022). Motion trajectory tracking and sway reduction for double-pendulum overhead cranes using improved adaptive control without velocity feedback. *IEEE/ASME Transactions on Mechatronics*, *27*(5), 3648–3659. https://doi.org/10.1109/TMECH.2021.3126665

[14] Shen, P.-Y., Schatz, J., & Caverly, R. J. (2021). Passivity-based adaptive trajectory control of an underactuated 3-dof overhead crane. *Control Engineering Practice*, *12*, 104834. https://doi.org/10.1016/j.conengprac.2021.104834

[15] Xia, J., & Ouyang, H. (2024). Amplitude saturated nonlinear output feedback controller design for underactuated 5-dof tower cranes without velocity measurement. *IEEE Transactions on Intelligent Transportation Systems*, *25*(8), 10206–10215. https://doi.org/10.1109/TITS.2024.3350056

[16] Huang, J., Wang, W., & Zhou, J. (2022). Adaptive control design for underactuated cranes with guaranteed transient performance: Theoretical design and experimental verification. *IEEE Transactions on Industrial Electronics*, *69*(3), 2822–2832. https://doi.org/10.1109/TIE.2021.3065835

[17] Yang, Y., Ye, X., Wen, B., Huang, J., & Su, X. (2023). Adaptive control design for uncertain underactuated cranes with nonsmooth input nonlinearities. *IEEE Transactions on Systems, Man, and Cybernetics: Systems*, *53*, 1074–1083. https://doi.org/10.1109/TSMC.2022.3192754

[18] Guo, Q., Chai, L., & Liu, H. (2023). Anti-swing sliding mode control of three-dimensional double pendulum overhead cranes based on extended state observer. *Nonlinear Dynamics*, *111*, 391–410. https://doi.org/10.1007/s11071-022-07859-9

[19] Yao, F., Tian, G., Wu, A., Duan, G.-R., & Kong, H. (2024). A high-order fully actuated system approach to control of overhead cranes. *IEEE/ASME Transactions on Mechatronics*, 1–12. https://doi.org/10.1109/TMECH.2024.3446670

[20] Lei, M., Wu, X., Zhang, Y., & Ke, L. (2023). Super-twisting disturbance-observer-based nonlinear control of the overhead crane system. *Nonlinear Dynamics*, *111*, 14015–14025. https://doi.org/10.1007/s11071-023-08596-3